Electronic Supplementary Information

Multiphasic *microgel-in-gel* materials to recapitulate cellular mesoenvironments *in vitro*

Dejan Husman[#], Petra B. Welzel[#], Steffen Vogler, Laura J. Bray, Nicole Träber, Jens Friedrichs, Vincent Körber, Mikhail V. Tsurkan, Uwe Freudenberg, Julian Thiele and Carsten Werner*

[#] contributed equally

Experimental Section

Hydrogel reaction mixture: A four-armed poly(ethylene glycol) each arm modified with an apopeptide (GCG**GPQGIWGQ**GCG, MW 1318 g mol^{-1}; synthesized in house), which includes an MMP-cleavable site (highlighted as bold text) was used in this study (starPEG-conjugate; molecular weight (MW): 15,500 g mol^{-1}). Heparin as the second gel component was functionalized with six maleimide groups (heparin conjugate; MW: 15,000 g mol^{-1}). Synthesis details are given in reference.[1] The mechanical properties of the hydrogel were adjusted by varying the molar ratio (γ) of the starPEG- and heparin-conjugate.

Microgel formation: Microgels were produced with the in-house designed co-flow device described below. 1 % (w/w) surfactant SPAN 85 (Sorbitan Oleate, Sigma-Aldrich, Munich, Germany) was added to the continuous phase of mineral oil (Drystrip Cover Fluid, GE Healthcare, Sigma-Aldrich) that was pumped through the device using a flow rate of 216 mL h^{-1}. The aqueous phase was injected into the device using two 1 mL BD syringes (Becton, Dickinson and Company, Heidelberg, Germany), one containing the heparin-conjugate and the other one containing the starPEG-conjugate both dissolved in phosphate buffered saline (PBS; flow rate: 1.6 mL h^{-1}). Both syringes were filled with a 'plug' of mineral oil (300 µL), before aspirating the hydrogel precursor solutions using flat tip/blunt Sterican® 21 G×7/8 0.8×22 mm needles (B. Braun, Melsungen, Germany) to minimize waste of both conjugates.
The two solutions were mixed by flowing through a P-860× Y-connector (IDEX, Illinois, USA) before entering the droplet forming glass capillary (diameter: 100 µm) of the co-flow device. In order to prevent gelation already in the capillary, gelation time was increased to ~3 minutes by reducing the pH of the starPEG-conjugate to a value of 4. After droplet formation, the water-in-oil (w/o) emulsion was passed through a 1.5 m long tubing (inner diameter: 3 mm, Tygon, Saint-Gobain, Paris, France) to give time for cross-linking within the droplets before reaching the collection vessel. The latter contained two phases, MilliQ water and a 10% (w/w) solution of SPAN85 in mineral oil, in order to stabilize the emulsion for as long as possible to enable complete curing of the droplets and prevent their aggregation/fusing. The cured droplets (microgels) were allowed to settle at the w/o interface, and the excess oil was removed. The microgels were broken out of the emulsion by centrifugation with MilliQ water, allowing the microgels to enter the aqueous phase and form a soft/semi-liquid pellet. The oil phase was removed with the supernatant aqueous phase, and the microgel dispersion was placed in a falcon tube for storage. 10% of 10 × PBS related to the final total volume was added at this point, to return the microgel dispersion to physiological osmolarity.
Glass capillary position x and composition γ of the hydrogel mixture were varied. Microgel size and mechanical properties (Young´s modulus) were determined as described below.

Preparation of microgel-in-gel materials: The microgels of a given *γ* prepared as described above were embedded in a bulk hydrogel with different mechanical properties (different *γ*). Therefore, the pre-formed microgels were suspended in the heparin-conjugate precursor solution, before mixing with the starPEG-conjugate solution. Apart from that, bulk hydrogels were prepared as described previously.[1] 30 µl *microgel-in-gel* constructs were casted onto a Sigmacote (Sigma-Aldrich) treated microscope slide.

Preparation of a 3D in vitro microgel-in-gel prostate cancer model: In the first step PC3 cells (compare *Cell culture*) were encapsulated in starPEG-heparin microgels with *γ* = 1: For cell embedding experiments DMEM (Dulbecco's Modified Eagle's Medium; Life Technologies) was used instead of PBS. PC3 cells at a final density of 1×10^6 mL^{-1} were mixed with the heparin-conjugate solution and co-injected with the starPEG-conjugate solution (adjusted to pH 4 as described above) into the co-flow device (flow rate 0.5 mL h^{-1} and continuous phase flow rate 216 mL h^{-1}) to form microgels (as described above). PC3 cells were cultured for up to 7 days within microgels to form cancer cell spheroids, which were visualized by means of brightfield microscopy. Viability was tested by life/dead staining and change of hydrogel mechanical properties due to cell-responsive degradation was studied by means of atomic force microscopy (AFM)-based nanoindentation (as described below).
In the second step, spheroid-containing microgels were embedded into the softer bulk hydrogel (*γ* = 0.63) prepared as follows: For the bulk hydrogel containing human umbilical cord endothelial cells (HUVECs) and mesenchymal stromal cells (MSCs) (10:1) the heparin-conjugate was further functionalized with 2 mol of a fibronectin-derived adhesion-mediating peptide sequence (H_2N-GCWGGRGDSP-$CONH_2$, RGD-SP; MW 990 g mol^{-1}; synthesized in house) per mole as described previously.[2, 3] Vascular endothelial growth factor (VEGF, PeproTech, Hamburg, Germany), stromal cell-derived factor 1 (SDF-1; Miltenyi Biotec, Bergisch Gladbach, Germany) and fibroblast growth factor 2 (FGF-2; Miltenyi Biotec) were added to stimulate HUVEC tube formation, and mixed at a concentration which corresponds to a final concentration of each 5 µg mL^{-1} per casted gel. 6×10^6 HUVECs and 6×10^5 MSCs per mL gel were each added into the heparin-conjugate/RGD-SP/growth factor mixture. After adding microgels containing PC3 spheroids and mixing with the starPEG-conjugate solution (γ = 0.63), 30 µl *microgel-in-gel* constructs were casted onto a Sigmacote-treated microscope slide as described above. 3D *in vitro microgel-in-gel* prostate cancer model systems were grown in 1.5 mL ECGM (endothelial cell growth medium, PromoCell, Heidelberg, Germany) at 37 °C and 5 % CO_2. After 5 days of co-culture, samples were fixed with 4 % PFA for immunofluorescence staining.

Co-flow device design and setup: The co-flow microfluidic device consists of three individual polycarbonate sections, one for the inlets, another one for the outlet and the third one for the droplet formation as can be seen in Figure S1. The separation allows exchange and thus flexibility in the geometry of the droplet forming section without constructing a whole new device. The geometry of the droplet forming middle-section can be controlled through shaping with precision machinery based on computer aided design (CAD). The sections align precisely due to steel dowels in the top/bottom sections, and are held together by four M8 hex screws. The top section contains inlets for the aqueous (top) and oil (side) phase tubing, which is secured to the device with HPLC screws. The continuous phase enters the device from the side inlet and flows downwards through the droplet forming middle section. The aqueous phase enters from the top inlet, flows through a glass capillary (diameter: 100 µm)

and is injected into the continuous phase stream in the cone-shaped droplet forming channel in the middle-section. In order to adjust the position of the glass capillary in flow direction, it was glued to the inside of a HPLC screw (using a two component epoxide glue, UHU, Baden, Germany), which can then be wound up or down.
Based on preliminary experiments (data not shown), the illustrated tapered cone-shape with drastic widening has been chosen as optimal for droplet formation. Different diameters of the narrowest point have been tested with this droplet forming geometry (including 200 µm, 300 µm, and 400 µm), and a 300 µm orifice diameter has been chosen as optimal.
The co-flow device was used on a custom-built stage (containing in-house machined components and assorted parts from Thorlabs, Lübeck, Germany). Droplet formation was imaged using an in-house assembled microscope (Olympus, objective 4×, Hamburg Germany) and a high-speed camera (MiroEx4; Vision Research, Baden-Baden, Germany) with a speed of 2475 fps directly at the glass capillary tip as well as further downstream. Flow rates of the aqueous phase were controlled by syringe pumps (PHD ULTRA; Harvard Apparatus, March-Hugstetten, Germany) and an in-house assembled nitrogen gas pressure system (N_2 gas and pressure valve; Alphagaz, Air Liquide, Düsseldorf, Germany) was utilized for adjusting continuous phase flow rates. Flow rates of the continuous oil phase were determined by measuring the mass of oil flowing out of the system over time at a constant N_2 pressure. Using the known density of mineral oil (0.85 g L^{-1}) (Drystrip Cover Fluid; GE Healthcare, Sigma-Aldrich) the corresponding flow rate was calculated.
In order to demonstrate that droplet size can be controlled and tuned by changing the relative position of the capillary in the co-flow device channel, water-in-oil droplets were produced. 1% (w/w) SPAN 85 (Sorbitan Oleate, Sigma-Aldrich) was added to the continuous phase and pumped through the device with a flow rate of 216 mL h^{-1}. MilliQ water as aqueous phase was injected with a flow rate of 0.5 mL h^{-1}, using a 1mL BD syringes (Becton, Dickinson and Company).
Size and size distribution of the water-in-oil droplets were obtained from brightfield microscope images (Olympus IX50, Olympus, Hamburg, Germany) using the 'measure length function' of Fiji (Image J, NIH, USA).

Glass capillary shaping: 1 mm diameter borosilicate glass tubes (World Precision Instruments, Florida, USA) were pulled using a glass capillary puller, (P97 Micropipette puller, Stutter Instruments, California, USA) The tapered glass capillary was then cut to the desired inner diameter using a microforge (MF-900 Microforge, Narishige, Japan) equipped with a platinum wire heater a microscope ocular with marked reticule.

Characterization of microgel size: The diameter of fluorescently labelled microgels (prepared with ATTO 488 or ATTO 647-labeled heparin-conjugate (1% of total heparin-conjugate mass) was determined by means of a widefield fluorescence microscope (Axiovert, Zeiss, Jena, Germany), using a 2.5× objective. Microgels were allowed to settle on the bottom of a flat-bottomed 24-well plate. An entire well of this plate was imaged using a tiling function and composited into a single image. This image was used to determine diameter and number of microgels with a macro written in Fiji/ImageJ. The average number of particles which can be counted using this method is ~2500.

Atomic force microscopy (AFM)-based nanoindentation (Colloid probe technique): AFM measurements were performed using a Nanowizard II AFM (JPK Instruments, Berlin, Germany) mounted on an inverted optical microscope (Observer.D1, Zeiss). Measurements

were conducted at 37°C with a Petri-Dish Heater (JPK Instruments) sample chamber. Tipless silicon nitride cantilever with a nominal spring constant of 80 mN m^{-1} (PNP-TR-TL-Au; Nanoworld) were utilized. Cantilevers were modified with silica beads (ø 10 µm, Kisker Biotec GmbH) as described.[4] Spring constants were calibrated before measurements using the equipartition theorem.[5]

To enable AFM measurements on a cross section of the *microgel-in-gel* construct, the multiphasic hydrogel samples were embedded into 1% agarose gels to facilitate handling. Subsequently, sections of high uniform thickness (700 µm) were cut by means of a vibratome (Leica VT 1000S, Wetzlar). To immobilize microgels and multiphasic hydrogel sections for AFM measurements, petri dishes (ø 40 mm, TPP) were coated with a 0.5% polyethyleneimine solution (Sigma Aldrich) for 20 min. Electrostatic interactions between the positively charged polyethyleneimine and the negatively charged heparin in the hydrogel materials effectively attached the hydrogel samples to the petri dish surface and prevented undesired movement of the samples during measurements. The hydrogel samples were fully hydrated and immersed in PBS. Under visual control, the bead-modified AFM cantilever was positioned above the center of the microgels or at the microgel-gel interface of the multiphasic materials, respectively. Force-distance curves were acquired in closed loop, constant height mode using 3 nN contact force and 5 mm s^{-1} approach/retract velocity. On microgels, 3 × 3 force-indentation maps were acquired on an area of 10 × 10 μm^2. At least 30 - 40 individual beads were probed per condition. For *microgel-in gel* samples, 20 × 20 force-indentation maps were acquired on an area of 100 × 100 μm^2. The data processing software provided by the AFM manufacturer (JPK Instruments) was used to extract the Young's modulus *E* from approach force-distance curves. The software applies a Hertz fit assuming a spherical indenter (**Equation 1**) with a radius (*R*) of 5 µm, and a Poisson's ratio (ν) of 0.5.

$$F = \frac{4}{3}\frac{E}{1-\nu^2}\sqrt{R}\delta^{\frac{3}{2}} \quad (1)$$

where *F* is the force and δ is the indentation.

Cell culture: The PC3 cell line was obtained from the American Type Culture Collection (ATCC; LGC Standards GmbH, Wesel, Germany), authenticated by the Deutsche Sammlung für Mikroorganismen und Zellkulturen (DSMZ, Braunschweig, Germany) and used for experiments before passage 10. PC3 cells were propagated in RPMI medium (Gibco, Germany) supplemented with 10% FBS and 1% penicillin/streptomycin solution (PS; Life Technologies, Darmstadt, Germany). HUVECs were isolated from umbilical cord veins as previously described,[6] and cultured on fibronectin-coated flasks. The endothelial cell growth medium (ECGM, PromoCell, Heidelberg, Germany) contained a supplemental mix with 2 % FBS (SupplementMix C-39215, PromoCell). MSCs were derived from healthy volunteer donors after informed consent (Universitätsklinikum Dresden) as described previously,[7] and cultured in DMEM supplemented with 10 % FBS, 1 % PS and 1 % of antibiotic/antimycotic solution 100× (Sigma Aldrich). HUVECs and MSCs were used within six passages.

Brightfield Microscopy: For standard analysis of cell cultures and for the examination of cells embedded into microgels, a brightfield microscope (Olympus IX50; greyscale phase contrast micrographs) in combination with Olympus cellSens software was used.

Live/Dead staining and widefield fluorescence microscopy: For testing prostate cancer cell viability after embedding into microgels and culturing for 7 days, a calcein/propidium iodide (green/red fluorescent) stain was performed. Supernatant cell culture medium was removed from microgels with embedded prostate cancer cells, and microgels were washed three times with sterile PBS. 200 µL of a 3 µM calcein solution together with 2.5-5.0 µM propidium iodide (both from Sigma-Aldrich, Germany) dissolved in PBS were added to stain the cells in a 48 well plate. Samples were incubated for 15 minutes at 37°C before imaging with a widefield fluorescence microscope (Axiovert, Zeiss).

Immunocytochemistry of microgel-in-gel co-cultures and confocal laser scanning microscopy: After fixation with paraformaldehyde (PFA, 4 %, Fluka, Deisenhofen, Germany) for 15 min, *microgel-in-gel* co-cultures were washed in PBS, blocked and permeabilized using 5% goat serum (Jackson Immuno Research Lab. Inc, USA) and 0.1% Triton X-100 (Sigma-Aldrich) in PBS and then directly immunostained. CD31 (Becton Dickson Biosciences, Heidelberg, Germany) and CK8 (Dianova, Hamburg, Germany) were detected using a dilution of 1:100 of primary antibody incubated overnight at 4º C. After washing, a secondary Alexa Fluor 488 antibody (Life Technologies) was applied to the samples at a 1:200 dilution in combination with phalloidin Alexa Fluor 633 (1:50 dilution; Life Technologies, Darmstadt, Germany) for actin staining overnight at 4ºC. For some samples phalloidin Alexa Fluor 488 was used. Afterwards, samples were washed and incubated with Hoechst 33342 nuclear dye (Life Technologies) at a concentration of 1 µg mL^{-1} in PBS for 30 min before visualization with a confocal laser scanning microscope (SP5, Leica Mikrosysteme Vertrieb GmbH, Wetzlar).

Statistical analysis: Data were analyzed using GraphPad Prism 6 (GraphPad Software Inc., USA) and presented as mean values ± standard error of mean.

Supporting Results and Figures

Control of the droplet size by adjusting the relative position of the capillary in the microfluidic co-flow device: By regulating the relative position of the glass capillary in the cone-shaped microchannel along the flow direction, as shown in Figure 1, S1 and S2, it is possible to control the diameter of the created monodisperse water-in-oil (w/o) droplets in a wide range (200 – 700 µm). Figure S2 illustrates six positions of the capillary with constant aqueous and oil flow rates of 0.5 mL h^{-1} and 216 mL h^{-1} respectively. As the capillary is moved deeper into the cone-shaped microchannel, the spacing between the capillary and the surrounding microchannel walls is decreased and with that the hydraulic diameter D_H of the microchannel that transports the continuous liquid flow to the droplet-forming microchannel geometry. In turn, this effectively alters the Capillary number (*Ca*) which, for droplet microfluidics, relates the magnitude of shear stress of a continuous liquid (oil) stream on an inner (aqueous) liquid jet to the surface tension of the outer phase, and thus determines the conditions for droplet breakup.[8] The Capillary number is defined as $Ca = \mu_c v_c/\sigma$, where μ_c is the dynamic viscosity of the continuous phase, σ the interfacial tension, and v_c the flow velocity of the continuous oil phase, which is a function of the orifice size and the volumetric flow rate.

From all parameters examined with respect on their influence on droplet diameter (surfactant concentration, flow rates and flow ratios, glass capillary orifice diameter, data not shown here) the control of relative capillary position was chosen as the easiest to perform during the course of an experiment.

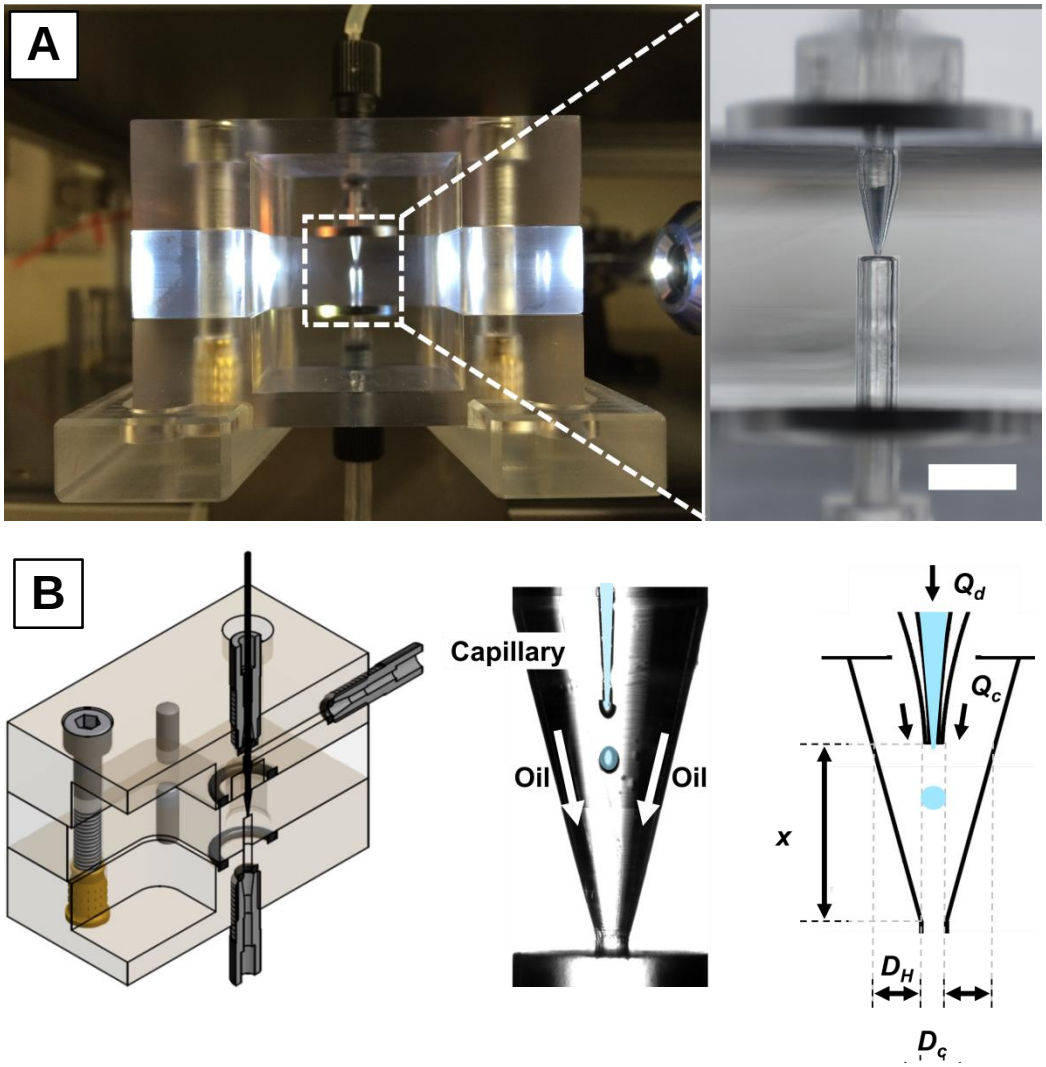

Figure S1. The in-house developed, co-flow microfluidic device constructed from micro-machined polycarbonate blocks to form a cone-shaped channel for the continuous phase with a movable glass capillary in its center for the aqueous phase. A) Device with imaging and microscope setup. A magnified view shows the droplet forming region of the device. The scale bar denotes 6 mm. B) A CAD generated drawing of the co-flow device cut in half, shows all inner channels. A magnified view of the droplet forming region during operation illustrates the cone-shaped channel for the oil phase, the glass capillary for the aqueous phase and the formed droplet (colored in blue). The scheme denotes all parameters which were evaluated for controlling droplet diameter *d* (data not shown). The design allows for varying the hydraulic diameter D_H and thus droplet diameter during the course of an experiment by simply regulating the relative position of the glass capillary *x* in flow direction in the cone-shaped channel without varying the volumetric flow rates of the liquids (Q_d (dispersed phase) and Q_c (continuous phase)) or the capillary orifice diameter D_c.

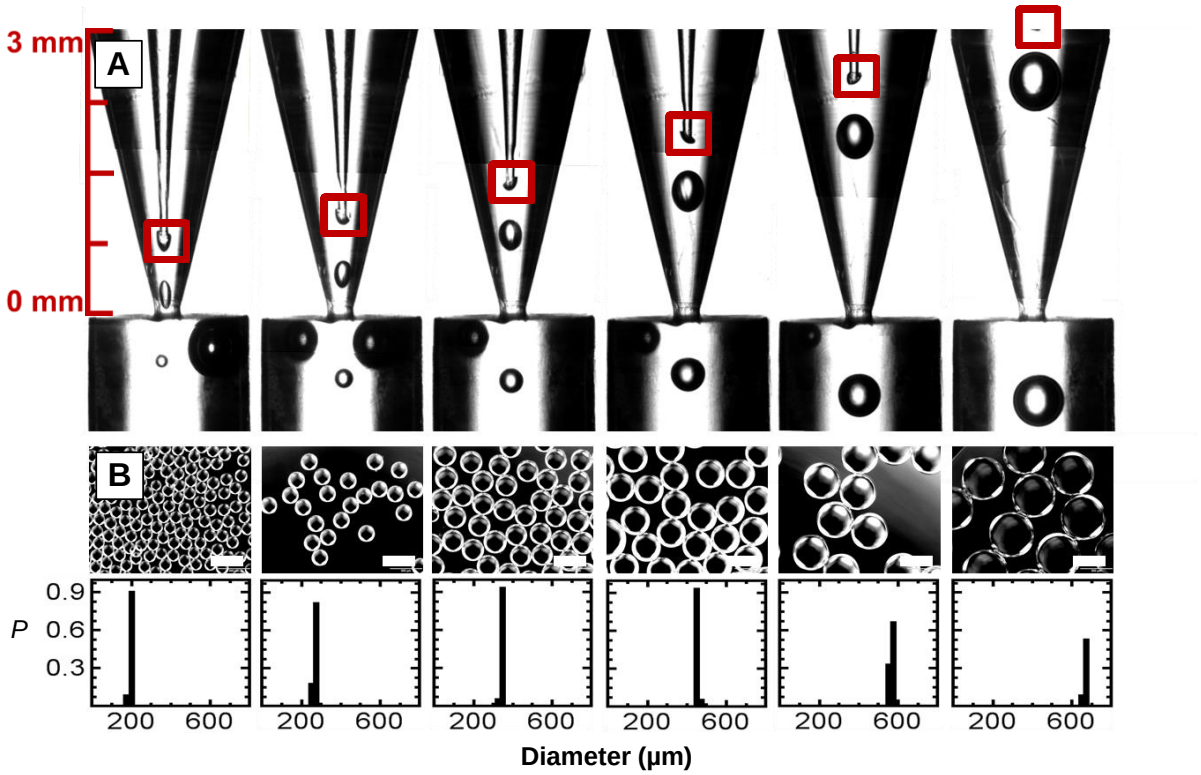

Figure S2. Formation of water-in-oil emulsions with varying droplet diameter employing the novel variant of microfluidic device composed of a cone-shaped droplet-forming channel with 300 µm orifice diameter and a glass capillary for droplet formation with 100 µm orifice diameter. Only the capillary position was altered to modulate droplet diameter (effectively altering the hydraulic diameter D_H). A) Glass capillary shown at six different positions at constant volume flow rates for the dispersed phase (0.5 mL h^{-1}) and the continuous phase (216 mL h^{-1}). B) Resulting monodisperse water-in-oil droplets with respective size distribution: fraction or percentage (P) of droplet diameters. Scale bar: 500 µm.

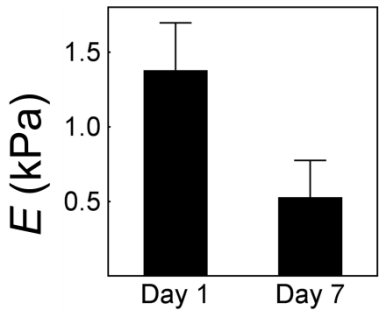

Figure S3. Incorporating an MMP-cleavable sequence into starPEG-heparin microgels allows for cell-induced degradation over time. Young's modulus of microbeads (γ = 1) with embedded PC3 cells at a density of 10^6/mL decreases over the course of 7 days culture.

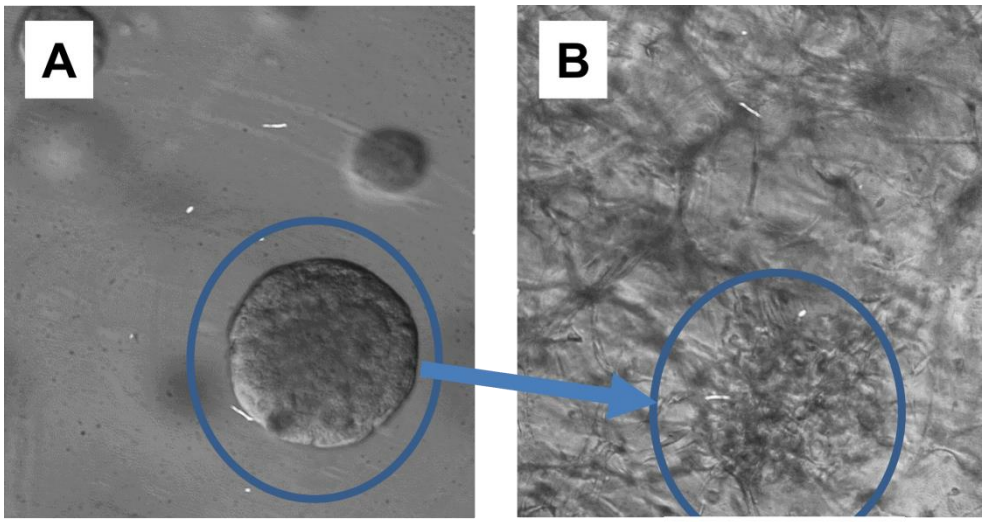

Figure S4. In a recently reported monophasic 3D prostate cancer model, human prostate cancer cells (PC3) share one common starPEG-heparin hydrogel matrix with the capillary network-forming co-culture of human umbilical cord endothelial cells (HUVECs) and mesenchymal stromal cells (MSCs). The chosen properties of the utilized starPEG-heparin hydrogel matrix had to be a compromise between the requirements of the two different cell populations. As invasive cancer cell types, such as PC3 cells, prefer to grow in stiffer microenvironments, whereas soft hydrogels were required for capillary endothelial cell network formation, PC3 spheroids had to be pre-formed separately in a stiff starPEG-heparin hydrogel (A), harvested and co-seeded together with HUVECs and MSCs in the soft starPEG-heparin hydrogel matrix (B). This procedure is less than ideal, as it alters the cancer-specific ECM formed during natural spheroid formation. Moreover, the transplant of a pre-grown PC3 cell spheroid, once placed inside of a soft hydrogel (supporting endothelial tubular formation), will result in a spheroid that will disintegrate into (migratory) single cells, changing the cellular phenotype (B), also compare[3].

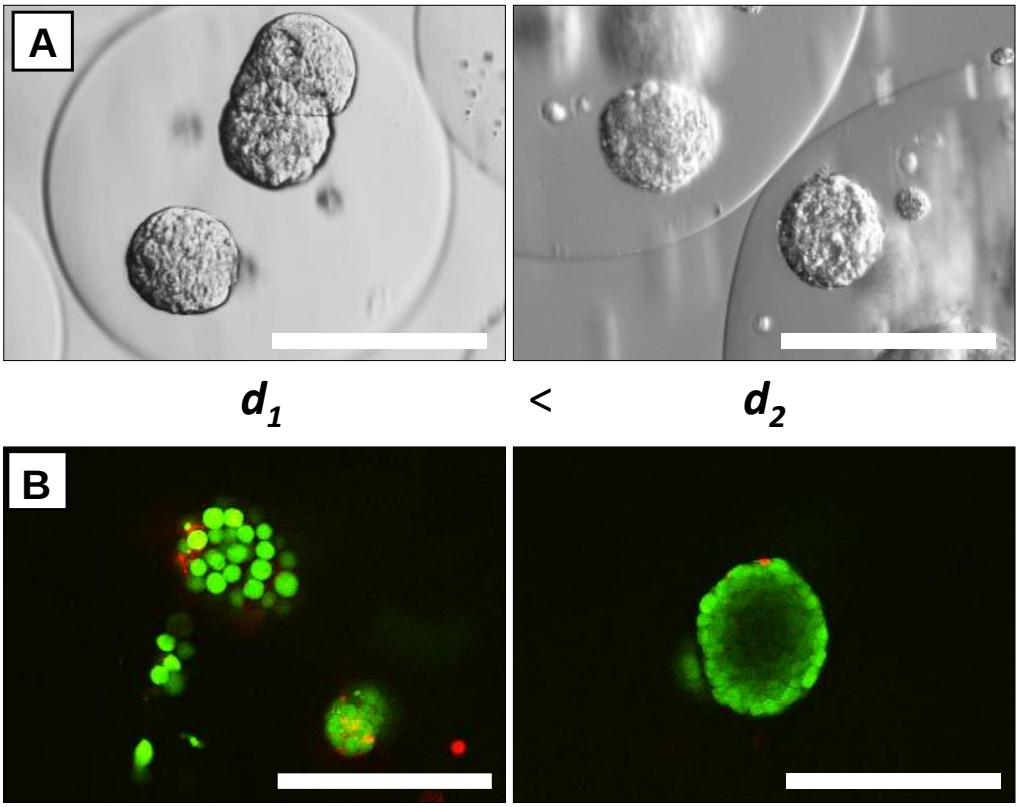

Figure S5. Brightfield microscopy was used to visualize PC3 cells embedded in the microbeads, which in the course of 7 days proliferated and eventually formed cancer spheroids as illustrated in Figure 2. A) Spheroid formation was observed in microgels of various sizes. B) Live/dead staining in combination with fluorescence microscopy of the prostate cancer spheroids showed mostly living cells (green) after 7 days (dead cells: red), indicating that the encapsulation using the co-flow microfluidic device was not detrimental to cell survival and continued proliferation. Left: 400 µm, right: 600 µm microgels. Scale bars: 200 µm.

1 M. V. Tsurkan, K. Chwalek, S. Prokoph, A. Zieris, K. R. Levental, U. Freudenberg and C. Werner, *Adv. Mater.,* 2013, **25**, 2606-2610.

2 A. V. Taubenberger, L. J. Bray, B. Haller, A. Shaposhnykov, M. Binner, U. Freudenberg, J. Guck and C. Werner, *Acta Biomater.* 2016, **36**, 73-85.

3 L. J. Bray, M. Binner, A. Holzheu, J. Friedrichs, U. Freudenberg, D. W. Hutmacher and C. Werner, *Biomaterials,* 2015, **53**, 609-620.

4 M. Krieg, Y. Arboleda-Estudillo, P. H. Puech, J. Käfer, F. Graner, D. J. Müller and C. P. Heisenberg, *Nat. Cell Biol.,* 2008, **10**, 429-436.

5 J. L. Hutter and J. Bechhoefer, *Rev. Sci. Instrum.,* 1993, **64**, 1868-1873.

6 J. R. Weis, B. Sun and G. M. Rodgers, *Thromb. Res.,* 1991, **61**, 171-173.

7 J. Oswald, S. Boxberger, B. Jorgensen, S. Feldmann, G. Ehninger, M. Bornhäuser and C. Werner, *Stem Cells,* 2004, **22**, 377-384.

8 A. R. Abate, J. Thiele and D. A. Weitz, *Lab Chip,* 2011, **11**, 253-258.